

Detail Modeling of High Speed Axial Flux Pm Generator

¹M. Sadeghierad, ¹H. Lesani, ¹H. Monsef and ²A. Darabi

¹Faculty of Elec. & Computer Engineering, Univ. of Tehran,
²Faculty of Elec. & Robotic Engineering, Shahrood Univ. of Tech.

Abstract: Recently more attention has been paid to the high-speed generator for its some merits, such as high power density, small size, etc. These high-speed operation impose stringent engineering design constrains not previously considered. Designing and the modeling of these high-speed axial flux generators (HSAFG) with leakage consideration is introduced in this paper. The FEM analysis is used for validation of this model.

Key words: High speed generator, axial flux permanent magnet, coreless stator, leakage flux

η : efficiency
 N_s : number of series coil per phase
P: number of poles
 λ (lambda): ratio of D_i to D_o
 D_o : outer diameter – R_o : outer radius (m)
 D_i : inner diameter – R_i : inner radius (m)
 D_{sh} : shaft diameter – R_{sh} : shaft radius (m)
 D_w : diameter of each wire of conductor (litz wire) (m)
 D_w : diameter of conductor (m)
 δ : ratio of area of PM to area of pole pitch
 R_{L1} : the PM leakage reluctance
 R_{L2} : between two PMs leakage reluctance
 R_{PM} : reluctance of the PM
 R_{g1} : reluctance of the air gap without fringing
 R_f : reluctance of the fringing
 R_g : reluctance of the air gap
 Φ_{PM} : Flux resource of PM
 B_r : residual flux density of PM
 B_g : flux density at air gap (T)
W: width of PM
x: start point of fringing
 μ_0 : air magnetic permeability
 μ_{rPM} : PM relative permeability
g : air gap (m)
 L_{PM} : length of PM (m)
 L_s : length of stator (m)
 L_{bi} : length of back iron (m)
 A_g : area of air gap (m²)
 A_{PM} : area of PM (m²)
 A_{st} : area of each wire of conductor (litz wire) (m²)
 δ_c : skin depth (m)
a: number of parallel path
 P_{out} : output power (kW)
 P_{loss} : power losses (kW)
 P_{mech} : mechanical losses (kW)
 P_{stator} : stator losses (kW)
 P_{rotor} : rotor losses (kW)

- P_{Br} : Bearing losses (kW)
- $P_{Windage}$: Windage (rotation) losses (kW)
- P_{vent} : ventilation losses (kW)
- P_{cu} : copper power loss (kW)
- P_{eddy_cu} : copper power loss (kW)
- ρ : air density (kg/m^3)
- μ_{air} : air viscosity coefficient (kg/ms)
- N_m : rotor speed (rad/s)
- ρ_{cu} : electrical resistivity ($\Omega.m$)
- V_{cu} : volume of copper (winding) (m^3)
- r_s : stator-winding resistance (Ω)
- i : full load current of machine (A)
- α : the temperature coefficient
- r_{s-dc} : stator dc resistance (Ω)
- r_{turn} : one turn of stator winding resistance (Ω)
- $r_s(\theta_1)$: resistance at a temperature θ_1 (Ω)
- $r_s(\theta_2)$: resistance at a temperature θ_2 (Ω)

μ_{cu} : relative magnetic permeability of copper

σ_{cu} : electric conductivity of copper

σ_{PM} : electric conductivity of PM

INTRODUCTION

The change of the energy usage structure and the potential market for distributed power resources make it promising to use the generation technology with high-speed axial-flux generators. High-speed axial flux PM generators are used in microturbines (a distributed power generation system). Distributed power generation system is used in remote and disastrous zones where grid power is unavailable (Holmes, A.S., *et al.* 2005). On the other hand, axial flux permanent magnet machines have been used increasingly with use of high-energy magnets for various applications. They have several unique features such as high efficiency, high power density, etc (Aydin, M., *at al.* 2002; Aglen,O., 2003). Fig. 1 shows this modular coreless high-speed axial-flux PM generator with three rotors and two stators. Due to the high rotor speed and high frequency of the stator flux variation, the design of a high-speed machine, is quite different from designing a conventional machine with low speed and low frequency. The following sections will discuss the design consideration and detail modeling of the HSAFG.

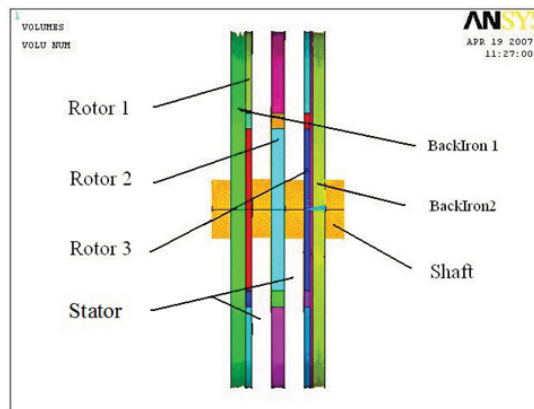


Fig. 1: Structure of The HSAFG

Rotor modeling:

Both electromagnetic and mechanical considerations have significant meaning for the rotor design of a high-speed machine compared to other structures. A PM rotor is preferred for more advantages such as simple structure, high power density, high efficiency, no excitation power loss, etc. (comparatively with induction machine, wound-field synchronous machine, BLDC machine, ...) (Sundaram, K.B., *et al.* 2005):

A. Permanent Magnet Non-linear Modeling:

A few material are common in PM machine, among them Nd-Fe-B and SmCo can be mentioned. Eddy current losses in Nd-Fe-B are less than SmCo, also performance to cost of Nd-Fe-B is higher than SmCo. So it is selected for this machine (Gieras J.F., *et al.* 2005). The model of PM is the reluctance with the mmf of PM (fig. 2).

$$R_{PM} = \frac{L_{PM}}{\mu_0 \mu_{rPM} A_{PM}} \tag{1}$$

$$mmf_{PM} = \phi_{PM} \times R_{PM} \tag{2}$$

$$\phi_{PM} = A_{PM} \times B_r \tag{3}$$

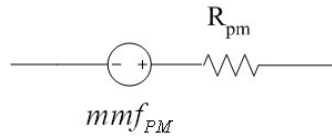


Fig. 2: Permanent magnet (PM) modeling Flux Leakage Modeling

B. Flux Leakage Modeling:

The model of self-leakage flux of PM (R_{L1}) and leakage flux between two PMs (R_{L2}) is considered as bellow (Wu, W., *et al.* 1995).

The self-leakage flux (R_{L1}) as two A and B path are shown in fig.3:

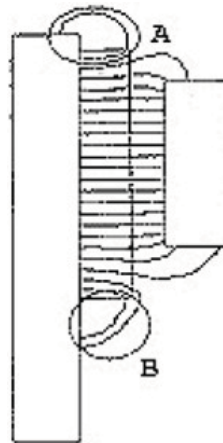


Fig. 3: Two path for self-leakage flux (for one PM)

$$R_{L1} = R_A \parallel R_B \tag{4}$$

That

$$R_A = \frac{2\left(\frac{P}{2}\right)}{\mu_0 \delta \left((D_i - L_{PM}) Ln \frac{L_{PM} + 2g}{L_{PM}} + 2g \right)} \quad (5)$$

$$R_B = \frac{9\left(\frac{P}{2}\right)}{\mu_0 \delta \left((3D_o + 2L_{PM}) Ln \frac{L_{PM} + 3g}{L_{PM}} - 6g \right)} \quad (6)$$

The leakage flux between two PMs (R_{L2}) is shown in fig. 4.

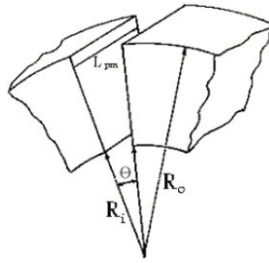


Fig. 4: Leakage flux between two Pms

$$R_{L2} = \frac{1}{\mu_0 Per_2} \quad (7)$$

$$Per_2 (\text{permiance}) = \frac{L_{PM} \times P}{2\pi(1-\delta)} Ln \frac{R_o}{R_i} \quad (8)$$

So the model of leakage flux in the HSAFG is obtained as fig. 5.

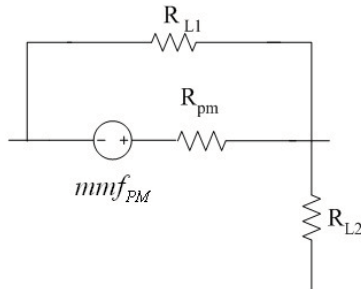


Fig. 5: Model of PM leakages.

C.n-linear 1Back iron Modeling:

The important nonlinear part of machine is the iron. There are two back iron at the both ends of machine on rotors. For modeling of back iron used the B(H) formula that is described in a FEM software (Sadeghierad, M. et al. 2008).

$$B(H) = \mu_0 H + \frac{2J_s}{\pi} \arctan\left(\frac{\pi(\mu_r - 1)\mu_0 H}{2J_s}\right) \quad (9)$$

The J_s is the factor that shown in the following fig. 6.

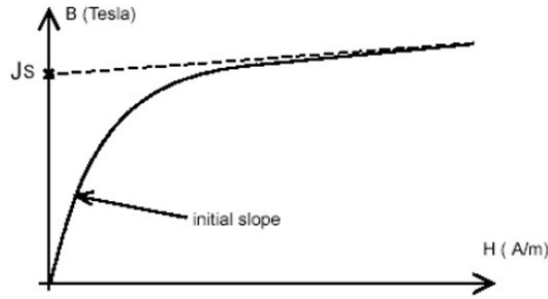


Fig. 6: Back iron modeling

So the model of back iron is a nonlinear reluctance (R_{iron}).

Stator Modeling:

For the stator design, the main problem is the high frequency of stator current and flux:

Stator Core Designing:

If the stator core materials and flux densities of a 60,000-rpm machine are the same for 3,000-rpm machine and the ratio of core losses per kilogram for two machines will be about 50, so the coreless stator is suggested [Caricchi, F. *et al.* 1998; Rong-Jie, *et al.* 2005; Lombard, N.F. and Kamper, M.J., 1999).

Stator Winding Designing

Due to high frequency current and high frequency magnetic field, the skin effect in stator winding should be considered. So, these wires are divided into several individually insulated strands to reduce this skin effect.

Stator and Air gap Modeling:

This coreless stator with two sides air gaps is modeled with the R_{g1} .

$$R_{g1} = \frac{(L_g + 2g)}{\mu_0 A_g} \tag{10}$$

Where:

$$A_g = \pi \left(\left(\frac{D_o}{2} \right)^2 - \left(\frac{D_i}{2} \right)^2 \right) \times \frac{1}{p} \tag{11}$$

Fringing effect Modeling:

For modeling the fringing effect (Fig. 7) four paths surrounding the PMs are assumed. The equivalent reluctance of air gap and stator is the parallel of R_{g1} and these four reluctances.

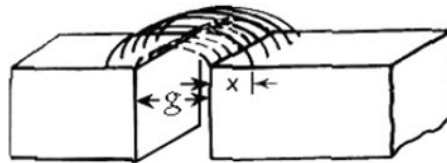


Fig. 7: Fringing effect.

The permeance of the fringing effect at each side of PM can be obtained according this formula:

$$Per_f(\text{permeance}) = \frac{W}{\pi} \ln \left(1 + 2 \left(\frac{x + x^2 + xg}{g} \right)^{0.5} \right) \tag{12}$$

$$R_f = \frac{1}{\mu_{rsm} \mu_r P_{erf}} \quad (13)$$

Loss calculation:

For efficiency calculation of model, power losses have to be intended. There are three losses: mechanical losses, stator losses, and rotor losses.

Mechanical losses:

These losses consist of bearing friction losses (P_{Br}), windage losses ($P_{Windage}$) rotation losses, and ventilation losses (P_{vent}) if there is a forced cooling system.

$$P_{mech} = P_{Br} + P_{Windage} + P_{Vent} \quad (14)$$

Bearing losses in comparing windage losses can be neglected. Windage losses (the power to overcome drag resistance of rotating disc) are calculated as:

$$P_{mech} = \frac{1}{2} c_f \rho (2\pi N_m)^3 (R_o^5 - R_{sh}^5) \quad (15)$$

That C_f the coefficient of drag for turbulent flow can be found as:

$$c_f = \frac{3.87}{\sqrt{Re}} \quad (16)$$

That Re the Reynolds number for a rotating disk with its outer radius is

$$Re = \rho \frac{R_o v}{\mu_{air}} = \frac{2\pi N_m \rho R_o^2}{\mu_{air}} \quad (17)$$

HSAFG machines are usually designed without a cooling fan so that the ventilation losses are equal zero. Stator losses:

These losses consist of core losses (P_{s-Fe}), copper losses (P_{cu}), eddy current (in wire) losses ($P_{eddy-cu}$).

$$P_{stator} = P_{s-Fe} + P_{cu} + P_{eddy-cu} \quad (18)$$

In the stator modeling section it is suggested to use a coreless stator. Therefore, there are not core losses. Copper loss (P_{cu}) is obtained by $i^2 r$ equation. The dc resistance is:

$$r_{dc} = \frac{R_{turn} \times N_s}{a} = \frac{\rho_{cu} \frac{L_{turn}}{N_{strand}} \times N_s}{a} = \frac{\rho_{cu} \times N_s \times (2 \times (\pi \times \frac{D_o + D_i}{2}) \times \frac{1}{P} + 2 \times (\frac{D_o - D_i}{2}))}{a \times N_{strand} \times A_{strand}} \quad (19)$$

But the resistance of the conductor is a function of the temperature:

$$r_s(\theta_2) = r_s(\theta_1)[1 + \alpha(\theta_2 - \theta_1)] \quad (20)$$

For ac resistance calculation, the skin effect in resistance can be considered according the skin depth (δ_c):

$$\delta_c = \frac{1}{\sqrt{(\pi f \mu_{cu} \sigma_{cu})}} \quad (21)$$

So, the effective resistance, which is a function of the frequency and skin effect, can be written as:

$$r_s(f) = r_{s,dc} \left[\frac{D_{st}}{\delta_c} \frac{\sinh 2(\frac{D_{st}}{\delta_c}) + \sin 2(\frac{D_{st}}{\delta_c})}{\cosh 2(\frac{D_{st}}{\delta_c}) - \cos 2(\frac{D_{st}}{\delta_c})} + \frac{2}{3} (D_{st}^2 - 1) \frac{D_{st}}{\delta_c} \frac{\sinh 2(\frac{D_{st}}{\delta_c}) - \sin 2(\frac{D_{st}}{\delta_c})}{\cosh 2(\frac{D_{st}}{\delta_c}) + \cos 2(\frac{D_{st}}{\delta_c})} \right] \quad (22)$$

At last the eddy current in wire ($P_{eddy-cu}$) because of magnetic filed high frequency is calculated by (Luk, P.C.K., and El-Hasan, T.S., 2005):

$$P_{eddy-cu} = \frac{(B_g \times 2 \times \pi \times f \times D_{st} \times 10^{-3})^2}{32 \times \rho_{cu}} \times V_{cu} \quad (23)$$

C. Rotor losses:

These losses consist of core losses (P_{r-Fe}), and PM losses (P_{PM}) rotation.

$$P_{rotor} = P_{r-Fe} + P_{PM} \quad (24)$$

Two back irons are rotate with the same speed as flux speed, so with this brilliant structure there are not core losses. Eddy current losses in the magnets are calculated by using Maxwell equations. However because of low σ_{PM} these losses can be neglected.

So, the efficiency is calculated by bellow formula:

$$\eta = \frac{P_{out}}{P_{out} + P_{loss}} \times 100 \quad (25)$$

That P_{loss} is equal to:

$$P_{loss} = P_{mech} + P_{stator} + P_{rotor} \quad (26)$$

Suggested Model And It's validation:

By collecting all parts models of machine (that obtained in rotor modeling and stator modeling sections) together, the simple magnetic model is obtained (fig. 8). This model with loss modeling (that described in chapter IV) presents a complete model of HSAFG.

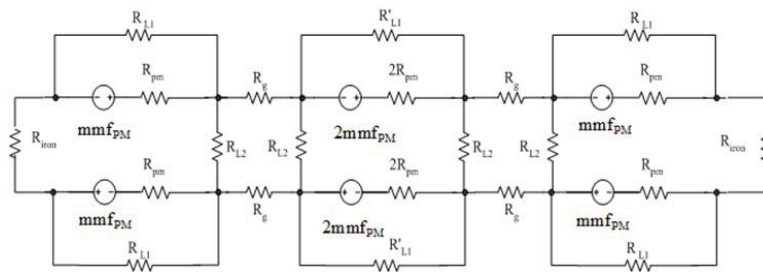


Fig. 8: Model of a coreless HSAFG

For validation of the suggested model, a FEM analysis is used. A HSAFG with 30,000 rpm, 30kW and 400V is designed by using the suggested model. The parameter of this machine is presented in appendix 1. According to the designing, the flux density of air gap is 0.437 and by FEM (fig. 9) is 0.419.

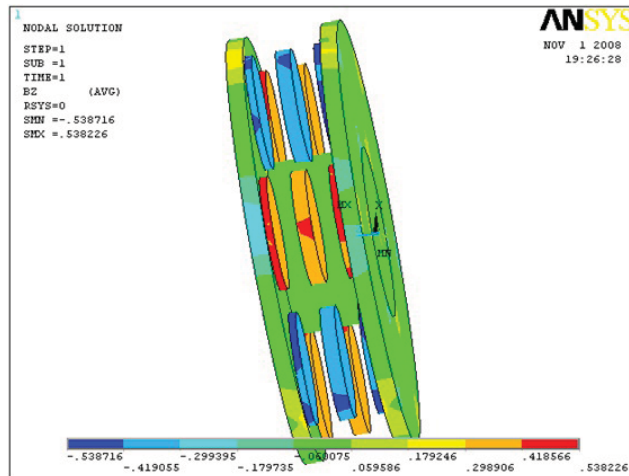


Fig. 9: Result of FEM

Conclusion: A design methodology for a modular High-speed axial-flux PM generator from first principles has been proposed. All power losses are considered as details. In this article, an accurate simple model of high-speed axial flux generator is presented. In this model leakage fluxes, fringing effect, nonlinear PMs and irons and all power losses are considered for the first time. At last this model is verified by the FEM analyses.

Appendix 1:

Main design parameters of the machine

Parameter	Value
P_{out} (W)	30,000
V (V)	400
N_m (rpm)	30,000
P	6
N_{serie}	21
D_o (m)	0.2437
L_s (m)	0.0024
L_{PM} (m)	0.0015
L_{bi} (m)	0.0067
g (m)	0.002
D_{strand} (m)	0.1
B_s (tesla)	1.2
R_s	0.0244
μ_{air}	0.000018
ρ	1.2
ρ_{cu}	1.678E-08

REFERENCES

Aydin, M., T.A. Surong Huang Lipo, 2002. A new axial flux surface mounted permanent magnet machine capable of field control. Industry Applications Conference. 37th IAS Annual Meeting, 2: 1250 - 1257.

Aglen, O., 2003. Back-to-back tests of a high-speed generator. Electric Machines and Drives Conference, IEMDC'03. IEEE International, 2: 1084 – 1090.

Caricchi, F., F. Crescimbeni, O. Honorati, G.L. Bianco, E. Santini, 1998. Performance of coreless-winding axial-flux permanent-magnet generator with power output at 400 Hz, 3000 r/min. Industry Applications, IEEE Transactions, 34(6): 1263 – 1269.

Gieras, J.F., R.J. Wang, M.J. Kamper, 2005. Axial Flux Permanent Magnet Brushless machine. Kluwer Academic Publisher.

Holmes, A.S., Guodong Hong; K.R. Pullen, Feb, 2005. Axial-flux permanent magnet machines for micropower generation. Microelectromechanical Systems, Journal of (IEEE JNL), 14(1): 54 – 62.

Lombard, N.F., M.J. Kamper, 1999. Analysis and performance of an ironless stator axial flux PM machine. Energy Conversion, IEEE Transactions, 14(4): 1051 – 1056.

Luk, P.C.K. and T.S. El-Hasan, 2005. Integrated design for a high speed permanent magnet axial flux generator. INTERMAG Conference, pp: 1083 – 1084.

Rong-Jie Wang, M.J. Kamper, K. Van der Westhuizen, J.F. Gieras, 2005. Optimal design of a coreless stator axial flux permanent-magnet generator. *Magnetics, IEEE Transactions*, 41(1-1): 55 – 64.

Sadeghierad, M., H. Lesani, H. Monsef and A. Darabi, 2008. Leakage Flux Consideration in modeling of High Speed Axial Flux PM Generator. *International Conference on Industrial Technology (ICIT08), IEEE International*, pp: 1-6.

Sundaram, K.B., j. Vaidya, L. Zhao, D. Acharya, C.H. Ham, J. Kapat and L. Chow, 2005. Analysis and Test of a High-Speed Axial flux permanent magnet Synchronous motor. *Electric Machines and Drives, IEEE International Conference on*, pp: 119 - 124.

Wu, W., E. Spooner, B.J. Chalmers, 1995. Design of slotless TORUS generators with reduced voltage regulation. *Electric Power Applications, IEE Proceedings*, 142(5): 337 - 343.